euspen's 24th International Conference & Exhibition, Dublin, IE, June 2024
www.euspen.eu

Fully compliant snap-through bistable gripper mechanism based on a pinned-pinned buckled beam

Loïc Tissot-Daguette[1], Simón Prêcheur Llarena[1], Charles Baur[1] and Simon Henein[1]

[1]*Instant-Lab – IMT – STI – EPFL*

loic.tissot-daguette@epfl.ch

Abstract

This paper presents a new planar flexure-based bistable two-jaw parallel gripper mechanism. The bistability of the mechanism is enabled by a pinned-pinned buckled beam suspended onto two cross-spring pivots. External energy is required only during the switching between the two stable states: open and closed jaws. This is particularly advantageous in gripping applications where power consumption is a limiting factor. Since it is based exclusively on flexure elements, this gripper mechanism is free from friction, wear and lubricant and is well suited for cleanroom environments, biomedical applications, or space environments. Another key feature is that the jaw opening/closing motion is based on fast snap-through transitions of the buckled beam, relying on an actuator motion which can be comparatively slow. This is highly beneficial for high-speed pick-and-place applications. Furthermore, the elastic decoupling between the actuator and the jaws allows the gripper to safely apply a limited output force to the grasped object, regardless of the force supplied by the actuator. In this article, the nonlinear load-deformation behaviors of the gripper are analytically modeled using Euler-Bernoulli beam theory and validated using finite element modeling. A prototype of the gripper mechanism with an external size of 10 mm x 35 mm x 85 mm was monolithically manufactured out of steel using wire electrical discharge machining. A voice coil actuator is integrated for actuation. The load-deformation characteristics, as well as the time to switch state, were measured on the prototype using a dedicated testbed. The experimental data are in good agreement with the theoretical models. The results show a stable gripping force of 1 N, a maximum stroke per jaw of 1.7 mm, and a state switching time (i.e., snap-through time) below 7 ms demonstrating high-speed gripping performances in comparison to state-of-the-art grippers.

Gripper, Mechanism design, Compliant mechanism, Flexures, Beam buckling

1. Introduction

Bistable grippers have the benefit of not requiring power to maintain the gripping and open states. This ability is extremely valuable in applications where energy consumption must be minimized and if the gripper may remain in closed or open state for extended periods of time, e.g., for drone perching [1] or for space applications [2]. Furthermore, if made fully compliant, bistable grippers are free from friction, wear and lubricant, and can thus be conveniently utilized in cleanroom or surgical environments [3].

In this work, a novel planar parallel fully compliant bistable gripper based on pinned-pinned buckled beam is presented. This bistable gripper exhibits rapid state switching created by snap-through. Thanks to the elastic decoupling between the actuation input and the jaws, the gripping output force is limited to a specific value. This is highly beneficial for preventing the damage of the grasped object [4]. The work will, first, describe the working principle of the gripper mechanism. Next, based on analytical modeling, a prototype is designed and fabricated. Experiment is then conducted to validate the design and modeling. Finally, a linear voice coil actuator is integrated to the bistable gripper to evaluate its dynamic performances.

2. Description and working principle

The ideal kinematics of the gripper mechanism is presented in Fig. 1a. Two parallelogram linkages are implemented to guide the jaws in translation. Both jaws are linked by an reverse-motion linkage to ensure that the jaws translate in opposite direction with the same displacement magnitude x_{out}. The rotating lever of the reverse-motion linkage is attached to a pin joint (called *output pivot*) and is connected to one extremity of an initially straight buckling beam. At its other extremity, the buckling beam is attached to a lever which is free to rotate around a second pivot joint (called *input pivot*). The two pinned extremities of the buckling beam can be brought togther by a displacement Δl using a preloading stage which is guided by a parallelogram linkage. This displacement causes the buckling beam to buckle, allowing the mechanism to exhibit a bistable behavior. When the gripper is in a stable position (open or closed), the gripper output state is maintained without requiring additional energy. The gripper state can be switched by actuating the input pivot. At specific values of the input angle θ_{in}, the mechanism reaches a snap-through instability where the output angle θ_{out} suddenly varies to close or open the jaws.

In order to make the gripper structure fully compliant, to be fabricated monolithically, the ideal joints in Fig. 1a are implemented by flexures, as seen Fig. 1b. The input and ouput pivots are embodied by cross-sping flexure pivots and parallelogram linkages by parallel leaf spring stages. The connecting rods of the reverse-motion linkage are replaced by simple blades. The precompression displacement Δl can be adjusted using a preloading screw (Fig. 1c). This adjustement can be used to tune the output jaw stroke x_{out} and the gripping force F_{out}. Furthermore, a lateral screw can be used to limit the jaw stroke to a specific value (see Figs. 1c and 1d). As we will see in Sec. 7.2, this second screw is used to reduce the vibration of the jaws.

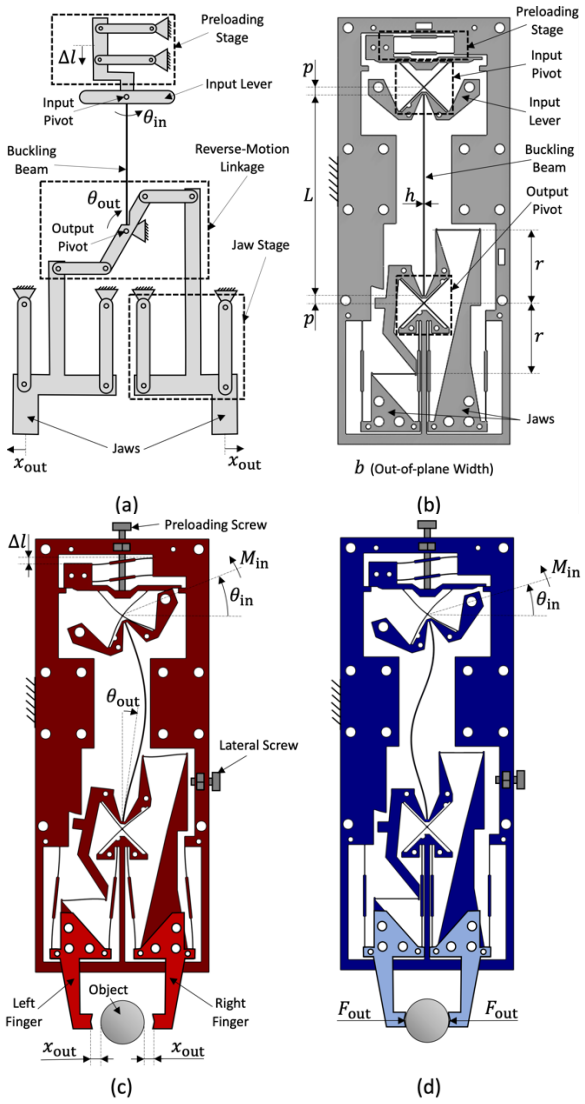

Figure 1. (a) Ideal kinematics of the gripper mechanism. Flexure-based gripper mechanism (b) in its fabricated position, (c) in open stable state and (d) in closed unstable state.

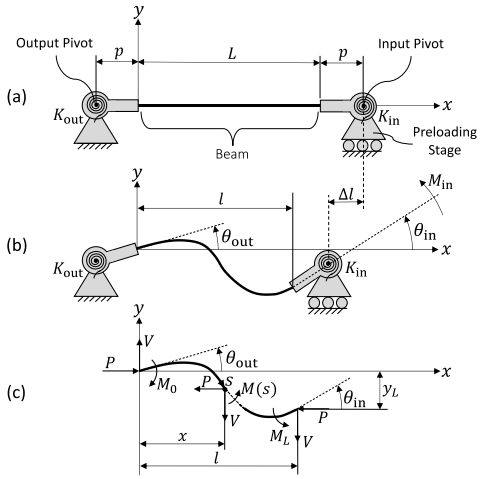

Figure 2. (a) As-fabricated, (b) deformed and (c) free-body diagram of the buckling beam.

3. Analytical model

A theoretical model is derived in order to characterize the nonlinear actuation behaviors of the gripper. To achieve that, the load-deflection characteristics of the buckling beam is first computed, then the gripping force and the jaw displacement are derived.

3.1. Buckled beam load-deflection characteristics

The schematic view of the buckling beam deflection is presented in Fig. 2. In this simplified schematics, the torsional springs K_{in} and K_{out} correspond to the equivalent angular stiffnesses resulting from the flexures at the input and output pivots, respectively. The buckled beam has a flexural rigidity EI and an initial length L. The distance p between the center of rotation of the pivots and the beam extremities is considered. Using the same modeling approach as in [5], the generic deflection y of a buckled beam can be expressed by:

$$y(s) = A\sin(ks) + B(\cos(ks) - 1) + Cs \tag{1}$$

where $k = \sqrt{P/EI}$ and s is the arclength position. After integrating the boundary conditions, i.e., $y'(s=0) \cong \theta_{\text{out}}$, $M_0 \cong K_{\text{out}}\theta_{\text{out}} + Vp - Pp\theta_{\text{out}}$, $y(s=L) \cong -p(\theta_{\text{out}} + \theta_{\text{in}})$ and $y'(s=L) \cong \theta_{\text{in}}$, in Eq. (1), the deflection parameters A, B and C are respectively given by:

$$A = \frac{-L\theta_{\text{in}}\left((1+2\bar{p})(kL)^2 + \varepsilon_{\text{out}}(\bar{p}kL\sin(kL) + 1 - \cos(kL))\right)}{kL\left(((\bar{p}+\bar{p}^2)(kL)^2 - \varepsilon_{\text{out}} + 1)kL\sin(kL) - ((kL)^2 + 2\varepsilon_{\text{out}})\cos(kL) + 2\varepsilon_{\text{out}}\right)} \tag{2}$$

$$B = -\frac{M_0}{P} = \frac{-L\theta_{\text{in}}\left((\bar{p}+2\bar{p}^2)(kL)^3 + \varepsilon_{\text{out}}(\bar{p}kL(\cos(kL)-1) - kL + \sin(kL))\right)}{kL\left(((\bar{p}+\bar{p}^2)(kL)^2 - \varepsilon_{\text{out}} + 1)kL\sin(kL) - ((kL)^2 + 2\varepsilon_{\text{out}})\cos(kL) + 2\varepsilon_{\text{out}}\right)} \tag{3}$$

$$C = \frac{V}{P}\frac{l}{L} \cong \frac{V}{P} = \frac{-\theta_{\text{in}}\left((\bar{p}^2(kL)^2 - \varepsilon_{\text{out}}\bar{p} - 1)kL\sin(kL) + (-2\bar{p}(kL)^2 + \varepsilon_{\text{out}})\cos(kL) - \varepsilon_{\text{out}}\right)}{((\bar{p}+\bar{p}^2)(kL)^2 - \varepsilon_{\text{out}} + 1)kL\sin(kL) - ((kL)^2 + 2\varepsilon_{\text{out}})\cos(kL) + 2\varepsilon_{\text{out}}} \tag{4}$$

where $\bar{p} = p/L$ and $\varepsilon_{\text{out}} = K_{\text{out}}/(EI/L)$. The end-shorting can be approximated with the following equation:

$$\Delta l \cong \frac{p}{2}\left(\theta_{\text{in}}^2 + \theta_{\text{out}}^2\right) + \int_0^L \frac{y'(s)^2}{2}ds = H(kL)\,L\theta_{\text{in}}^2 \tag{5}$$

where from [5]:

$$H(kL) = \frac{(\bar{A}^2+\bar{B}^2)(kL)^2}{4} + \frac{(\bar{A}^2-\bar{B}^2)kL\sin(2kL)}{8} + \frac{\bar{A}\bar{B}kL(\cos(2kL)-1)}{4} + \bar{A}\bar{C}\sin(kL) + \bar{B}\bar{C}(\cos(kL)-1) + \frac{\bar{C}^2}{2} + \frac{\bar{p}}{2}((\bar{A}kL + \bar{C})^2 + 1) \tag{6}$$

where the deflection parameters are normalized as follows: $\bar{A} = A/(L\theta_{\text{in}})$, $\bar{B} = B/(L\theta_{\text{in}})$ and $\bar{C} = C/\theta_{\text{in}}$. By rearranging Eq. (5), the input angle can be evaluated as a function of kL:

$$\theta_{\text{in}} = \pm\sqrt{\frac{\Delta l}{L}}\sqrt{\frac{1}{H(kL)}} \tag{7}$$

The input moment can be written as follows:

$$M_{\text{in}} \cong M_L + Vp - Pp\theta_{\text{in}} + K_{\text{in}}\theta_{\text{in}} = \frac{EI}{L}((kL)^2(\bar{p}(\bar{C}-1) - \bar{A}\sin(kL) - \bar{B}\cos(kL)) + \varepsilon_{\text{in}})\theta_{\text{in}} \tag{8}$$

where $M_L = EIy''(s=L)$ and $\varepsilon_{\text{in}} = K_{\text{in}}/(EI/L)$ is the relative input stiffness.

3.2. Output force-displacement characteristics

Considering that the reverse-motion linkage has a lever length r (see Fig. 1b), the force-displacement characteristics of the jaws is related to the moment and angle of the buckling beam output pivot as follows:

$$F_{\text{out}} = \frac{M_0 - Vp}{2r} = -\frac{EI}{L}\frac{(\bar{B}+\bar{C}\bar{p})(kL)^2\theta_{\text{in}}}{2r} \quad (9)$$

$$x_{\text{out}} \cong r\theta_{\text{out}} = r(\bar{A}kL + \bar{C})\theta_{\text{in}} \quad (10)$$

Note: While the gripper is in closed and open states, F_{out} and x_{out} are respectively assumed to be null.

4. Prototype design

Using the analytical model, a flexure-based mesoscale embodiment of the compliant structure was designed and manufactured with wire-cut electrical discharge machining (EDM) process. The selected material of the compliant structure is steel (Böhler K390), with a yield strength $\sigma_y = 2300$ MPa and Young's modulus $E = 220$ GPa. The cross-spring pivots at the input and output of the buckling beam have equal dimensions. Their angular stiffness can be calculated from [6] as $K_{\text{p}} = 2Ebh_{\text{p}}^3/(3L_p)$, where h_{p} is the thickness and L_{p} is the total diagonal length of the crossed blades. The input angular stiffness K_{in} is simply equal to K_{p}. In open state, the output angular stiffness constant $K_{\text{out,open}}$ is evaluated from Finite Element Method (FEM), to make modeling simpler. In closed state, $K_{\text{out,closed}}$ tends to infinity assuming that the object and the fingers are considerably stiff. The parameters of the fabricated gripper mechanism are summarized in table 1.

Table 1 : Design parameters (see Figs. 1 and 2)

	Parameter	Value
Mechanism width	b	10 mm
Preloading stage	Δl	1.25 mm
Buckling beam	h L p	150 µm 40 mm 2 mm
Cross-spring pivots	h_{p} L_{p}	60 µm 11.2 mm
Reverse-motion linkage	r	14 mm
Equivalent angular stiffnesses	K_{in} $K_{\text{out,open}}$	28.3 Nmm/rad 211 Nmm/rad

5. FEM and experimental characterization

A 2D static FEM study is carried out on Comsol Multiphysics 5.4 to verify the analytical model and the gripper design. The nonlinear load-deformation characteristics of the gripper are simulated by varying the input pivot angle θ_{in}. Deflection solutions of the study are illustrated in Figs. 1c and 1d and the FEM data are reported in Sec. 7.1.

The load-deformation characteristics of the gripper prototype are experimentally evaluated using a dedicated test bench, see Fig. 3. The setup includes a manual micrometer linear stage to push the mechanism input lever by an angle θ_{in} through a force sensor (Kistler Model 9207) in order to measure the applied input torque M_{in}. The angle θ_{in} and the displacement x_{out} of one of the jaws are recorded by laser displacement sensors (Keyence Model LK-H082). A second identical force sensor placed in-between the two jaws measures the gripping force F_{out}. The mechanism is characterized, for both opening and closing transitions, from the corresponding stable state until snap-through. Data acquisition is performed after each increment of the linear stage position when the system is steady in order to assess quasi-static measurements.

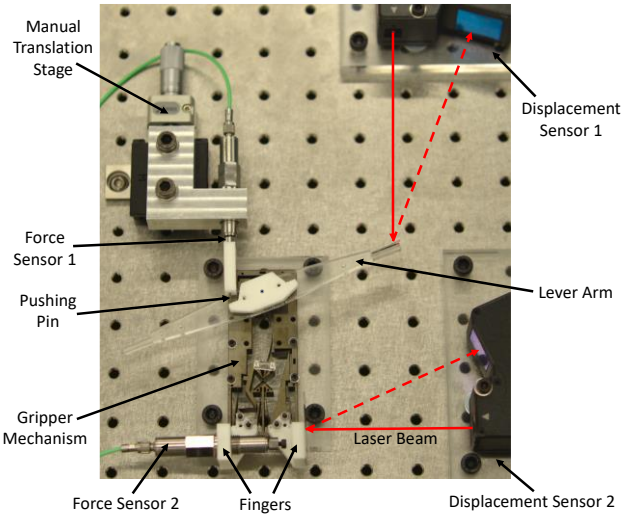

Figure 3. Test bench used to characterize the gripper mechanism.

6. Actuator integration

Based on the gripper actuation requirements obtained from the models and the experiment, we have selected a linear voice coil motor (Moticont LVCM-025-022-01) for the actuation of the gripper input pivot (Fig. 4). A 3D-printed monolithic compliant coupling mechanism is based on a parallel leaf spring stage to guide the coil holder with respect to its fixed frame. A flexure-based connecting rod and a lever arm are used to convert the linear motion of the coil into a rotation to angularly actuate the input pivot. The proposed control strategy consists in applying a constant electrical current in the voice coil such that the applied moment exceeds the opening and closing critical moments (Fig. 5) in order to switch the gripper states.

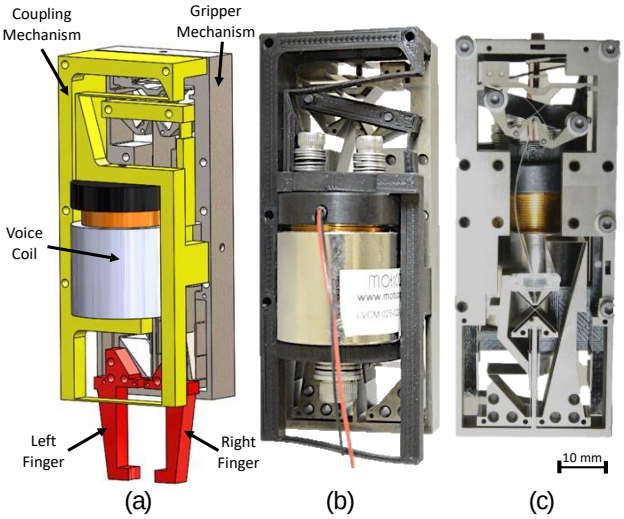

Figure 4. Assembly of the bistable gripper with voice coil actuator. (a) Schematic (with mounted fingers), and photographs with (b) front and (c) back views.

7. Results and discussion

7.1. Actuation characteristics

The analytical results of the actuation characteristics as well as the ouput force and displacement are illustrated in Fig. 5 (where the blocking effect of the lateral screw is not taken into account). Using Eqs. (7)-(10), the analytical parametric curves are traced out as the parameter kL ranges from 1.4π (near the closed stable state) to 2.4π (at the unstable position) and from 1.3π (near the open stable state) to 2.2π (at the unstable position) for the closed and open gripper states, respectively. The FEM and experimental data are added in Fig. 5 to evaluate the

accuracy of the analytical model. Since the error between the analytical and FEM models is bounded within 5%, the analytical modeling derived in Sec. 3 is validated. Some discrepancies between the experimental data and the models (15% maximum difference) are assumed to be due to manufacturing tolerances and measurement errors.

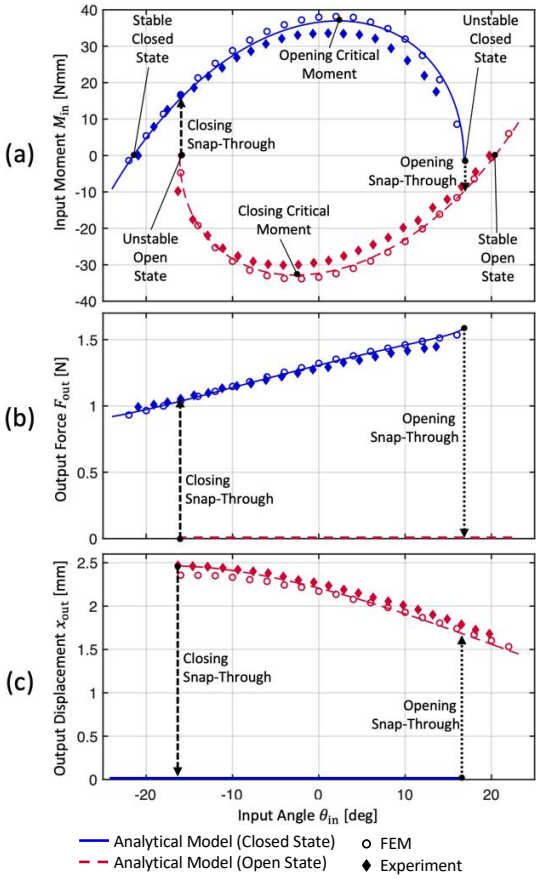

Figure 5. (a) The input moment, (b) the output force and (c) the output displacement as a function of the input angle.

As can be observed in Fig. 5(a), the gripper is in a stable equilibrium at $\theta_{\text{in}} = 20°$ and $\theta_{\text{in}} = -21°$ and reaches unstable states at $\theta_{\text{in}} = -16°$ and $\theta_{\text{in}} = 17°$, when open and closed, respectively. When the unstable gripper states are outreached, snap-through under angle control occurs. This causes hysteresis in the actuation. During both closing and opening sequences, the input moment M_{in} reaches a maximum magnitude, see Fig. 5(a). In order to switch the gripper state, the actuator must hence be able to apply these critical moment values. The snap-through transitions lead to discontinuous changes at the gripper output as can be see in Figs. 5b and 5c. In stable closed and open states, F_{out} and x_{out} are constant and equal to 1 N and 1.7 mm, respectively. During actuation to switch the gripper state, F_{out} and x_{out} increase until they reach a limited value, just before snap-through, of 1.6 N and 2.5 mm, respectively. This shows that the gripper has force limitation properties and that the gripper will continuously apply a force on the gripping part during the opening, and will always be open during the closing transition.

7.2. Dynamic behavior

The dynamic response of the gripper prototype actuated by the voice coil is recorded with a high-speed camera (IDT NX4-S3) at a frame rate of 5000 Hz. Based on the video frames and timing, table 2 reports the durations of the *actuation* (when the actuator starts to move until snap-through occurs), *snap-through* (until the gripper reaches its final state), and *stabilization* (until the gripper is stable within 10% error with respect to its final state). The video of the dynamic testing is available here: https://youtu.be/LWhnJjIXFwo. In this experiment, the lateral screw is used to limit the jaw displacement to $x_{\text{out}} = 1.4$ mm. Without the lateral screw, the opening stabilization time is in the order of 1 s, which is impractical for high-speed pick-and-place applications. Indeed, the jaws would oscillate around the stable open position with low energy disspation (due to the absence of solid friction in flexure mechanisms). Even when the lateral screw is used, some vibrations of the flexures remain at the output. To further reduce the stabilization time, damping systems would need to be added to the gripper output.

Snap-through allows the gripper to advantageously, change states rapidly. Yet, impacts on the object to be grasped might be relatively important. For brittle objects, one could consider adjusting the compliance of the fingers to limit the shock level.

Because the gripper input and output are substantially decoupled until snap-through (see Fig. 5), the operations can be cascaded. For instance, the actuation can begin before the jaws are fully stabilized.

Table 2 : Time durations of the gripper actuation sequences

	Sequence	Time [ms]
Opening	Actuation	21.6
	Snap-through	5.4
	Stabilization	28.8
Closing	Actuation	26.4
	Snap-through	6.6
	Stabilization	4.2

8. Conclusion

This work presents a novel fully compliant parallel gripper based on pinned-pinned buckled beam to achieve bistability. This bistable gripper, powered by a voice coil, demonstrates rapid opening and closing motions while requiring no additional energy to maintain its open or closed state. Thanks to the elastic decoupling between the actuation and the jaws, the gripping force is advantageously limited. In this paper, an EDM-wire cut monolithic gripper is designed, modeled and fabricated. Experimental results are in good agreement with the established models, and exhibit a maximum total jaw aperture of 3.4 mm and stable gripping force of 1 N. Dynamic testing shows a snap-through time in the order of 7 ms for both closing and opening sequences. Future work will include designing and integrating Shape Memory alloy (SMA) actuators to actuate this gripper with minimized time response and compact volume.

Acknowledgements

This project is funded by the Swiss Innovation Agency (Innosuisse Project no.: 51060.1 IP-ENG).

References

[1] Zhang H, Lerner E, Cheng B and Zhao J 2021 Compliant bistable grippers enable passive perching for micro aerial vehicles *IEEE ASME Trans. Mechatron.* **26** 2316-2326

[2] Zhang Y, Quan J, Li P, Song W, Zhang G, Li L and Zhou D 2023 A flytrap-inspired bistable origami-based gripper for rapid active debris removal *Adv. Intell. Syst.* **5** 2200468

[3] Lassooij J, Tolou N, Tortora G, Caccavaro S, Menciassi A and Herder J 2012 A statically balanced and bi-stable compliant end effector combined with a laparoscopic 2DoF robotic arm *Mech. Sci.* **3** 85-93

[4] Liu Y, Zhang Y and Xu Q 2017 Design and control of a novel compliant constant-force gripper based on buckled fixed-guided beams *IEEE ASME Trans. Mechatron.* **22** 476-486

[5] Tissot-Daguette L, Schneegans H, Thalmann E, Henein S 2022 Analytical modeling and experimental validation of rotationally actuated pinned–pinned and fixed–pinned buckled beam bistable mechanisms *Mech. Mach. Theory* **174** 104874

[6] Cosandier F, Henein S, Richard M, Rubbert L 2017 *The art of flexure mechanism design* EPFL Press Lausanne